5-1-1996

# Applications of the normal-incidence rotating-sample ellipsometer to high- and low-spatial-frequency gratings

Y. Cui

R. M.A. Azzam
*University of New Orleans*, razzam@uno.edu

TECHNICAL NOTE

# Applications of the normal-incidence rotating-sample ellipsometer to high- and low-spatial-frequency gratings

Y. Cui and R. M. A. Azzam

The normal-incidence rotating-sample ellipsometer is an instrument that can be used to characterize grating surfaces from the measured ratio $\rho$ of complex reflection coefficients $r_y/r_x$ of light polarized perpendicular and parallel to the grating groove direction. Experimental results at different wavelengths for different gratings with spatial frequencies from 150 to 5880 grooves/mm are presented. The groove depth of the 5880-grooves/mm gold-coated grating can be estimated from the measured $\rho$ and rigorous grating theory. © 1996 Optical Society of America

## 1. Introduction

The normal-incidence rotating-sample ellipsometer (NIRSE) was introduced to measure the ratio of complex reflection coefficients $\rho = r_y/r_x$ of anisotropic surfaces,[1–3] where $x$ and $y$ represent two orthogonal linear polarizations of light along principal directions of the surface. Surface-relief gratings are highly anisotropic, and the complex reflection coefficients $r_x$ and $r_y$ of the grating determine the amplitude and phase changes for zero-order reflection of incident light polarized parallel and perpendicular to the grating grooves. Thus this technique offers a useful tool for grating metrology based on recent advances in rigorous and approximate grating theories.[4–7] From grating theory and measured ratios of complex reflection coefficients valuable information about the grating groove depth, groove profile, and surface films may be obtained.

In this paper we present experimental results of $\rho$ for different gratings with spatial frequencies from 150 to 5880 grooves/mm at visible wavelengths from 543.5 to 632.8 nm. Experimental results for the 5880-grooves/mm grating are compared with theoretical calculations.

The authors are with the Department of Electrical Engineering, University of New Orleans, Lakefront, New Orleans, Louisiana 70148.

Received 7 September 1995; revised manuscript received 7 November 1995.
0003-6935/96/132235-04$10.00/0


## 2. Description of the Normal-Incidence Rotating-Sample Ellipsometer

Figure 1(a) shows the arrangement of the NIRSE. Light source L is a He–Ne laser at 632.8 or 543.5 nm or an argon-ion laser-pumped wavelength-tunable dye laser system.[8] The monochromatic light beam from L is linearly polarized by a Glan–Thompson polarizer P, whose transmission axis $t$ is vertical as shown in Fig. 1(b), and falls perpendicularly onto the surface of reflection grating G. The zero-order beam reflected back from G passes through polarizer P again (which now acts as an analyzer) and is reflected to photodetector $D_1$ by beam splitter $BS_1$. Higher-order beams (if present) are blocked and do not contribute to the received signal. A reference signal is obtained by a second beam splitter $BS_2$ and photodetector $D_2$ to monitor the input light intensity variation. The grating is mounted on the shaft of a stepping motor SM, whose rotation axis coincides with the incident light beam axis. The surface normal of $BS_1$ forms a small angle $\delta$ ($\sim 1°$) with respect to the optical axis to reduce the effect caused by any misalignment of the rotation axis and the grating normal.[9] Two Cartesian coordinate systems $(x, y)$ and $(p, s)$ are shown in Fig. 1(b). The $x$–$y$ coordinate system rotates with the grating, where $x$ and $y$ are parallel and perpendicular to the grating groove direction, respectively. The $p$–$s$ coordinate system is fixed in space, where $p$ and $s$ are parallel and perpendicular to the transmission axis $t$ of polarizer P, respectively. The grating rotates in 1° steps.

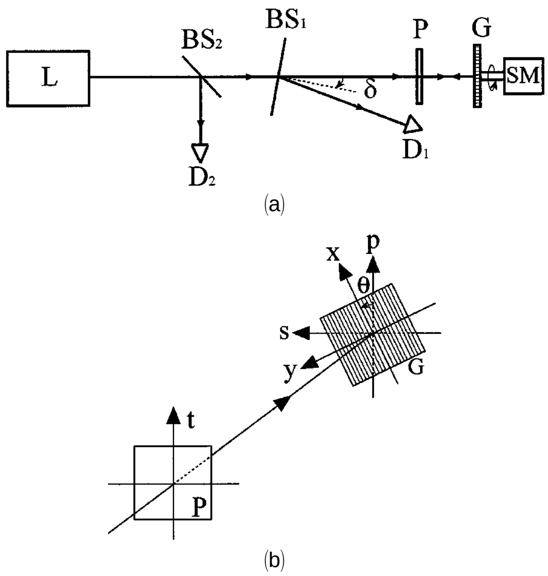


Fig. 1. (a) Experimental setup of the NIRSE: L, light source; $BS_1$, $BS_2$, beam splitters; $D_1$, $D_2$, silicon photodetectors; P, Glan–Thompson polarizer; G, grating sample; SM, stepping motor. (b) Relative position of the rotating $x$–$y$ and space-fixed $p$–$s$ Cartesian coordinate systems. P and G are the same as in (a).

### 3. Results and Analysis

The output electrical signal from $D_1$ is normalized by the reference signal from $D_2$. The normalized signal $\mathscr{T}_D$ is a periodic function of the grating rotation angle θ, which is governed by the anisotropic reflection properties of G, and is Fourier analyzed to get ρ. Detailed derivations can be found in Ref. 2. Signal $\mathscr{T}_D$ as a function of grating rotation angle θ can be written as

$$\mathscr{T}_D = c[(1 + \tfrac{1}{2}|\eta|^2) + 2\,\mathrm{Re}(\eta)\cos(2\theta) + \tfrac{1}{2}|\eta|^2\cos(4\theta)], \tag{1}$$

where $c$ is a constant independent of θ and $\eta = (r_x - r_y)/(r_x + r_y)$.

Misalignment of the stepping motor and grating affects signal $\mathscr{T}_D$ in such a way that only odd harmonics are added to the signal.[10] Therefore the even harmonic coefficients, which contain information about ρ, can be extracted using Fourier analysis. We include the small odd harmonics in fitting the signal $\mathscr{T}_D$ but use only the second and fourth harmonic coefficients in calculations. Let $\eta = \eta_1 + j\eta_2$. A least-squares fit of signal $\mathscr{T}_D$ gives

$$\mathscr{T}_D = a_0 + a_2\cos(2\theta) + a_4\cos(4\theta). \tag{2}$$

Then η can be determined by

$$\eta_1 = \frac{a_2}{2(a_0 - a_4)},$$
$$\eta_2 = \frac{1}{2(a_0 - a_4)}(8a_0a_4 - 8a_4{}^2 - a_2{}^2)^{1/2}, \tag{3}$$

and the ratio of complex reflection coefficients ρ can

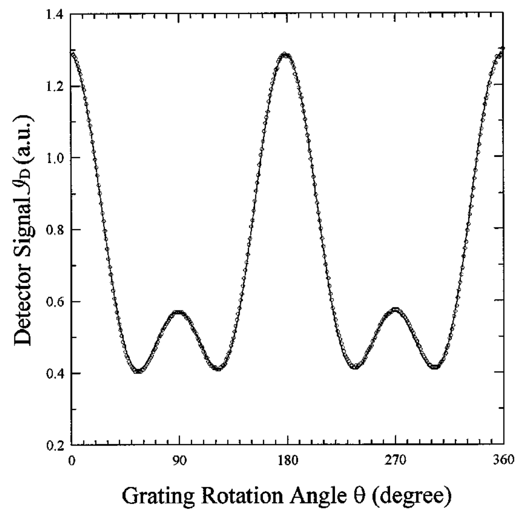


Fig. 2. Normalized detector signal $\mathscr{T}_D$ as a function of grating rotation angle θ. The circles are experimental data points and the solid curve is the least-squares fit curve.

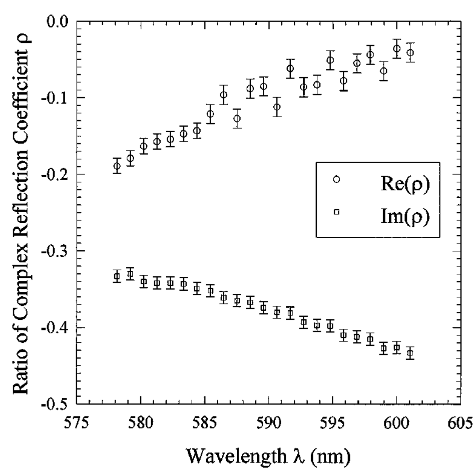


Fig. 3. Re(ρ) and Im(ρ) as functions of wavelength λ for a 600-grooves/mm aluminum-coated grating.[11] The standard deviation of the measurement varies from 0.015 to 0.025 when a dye laser is used as the light source.

**Table 1. Values of ρ Measured by the NIRSE for Different Gratings at Three Different Wavelengths[a]**

| Grating Frequency Grooves/mm | λ = 543.5 nm | λ = 590 nm | λ = 632.8 nm |
|---|---|---|---|
| 150 (11) | 0.956–$j$0.046 | NA | 0.945–$j$0.171 |
| 600 (11) | −0.676–$j$0.668 | −0.085–$j$0.374 | −0.047–$j$0.614 |
| 1200 (11) | 0.080–$j$0.419 | 0.146–$j$0.287 | 0.359–$j$0.220 |
| 600 (17) | NA | 0.699–$j$0.203 | 0.741–$j$0.108 |
| 1200 (17) | NA | 0.469–$j$0.138 | 0.533–$j$0.128 |
| 400 (12) | −0.324–$j$0.276 | 0.127–$j$0.184 | 0.360–$j$0.161 |
| 5880 (12) | 0.747–$j$0.318 | 0.932–$j$0.183 | 0.960–$j$0.202 |

[a]The number in parentheses after the grating spatial frequency identifies the vendor as given in the list of references.
NA, not available.

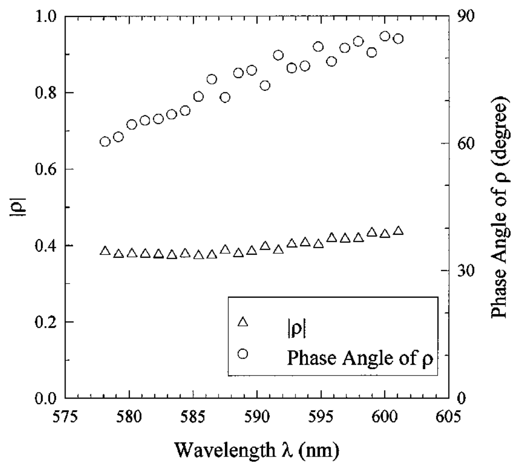


Fig. 4. Absolute value and phase angle of ρ as a function of wavelength λ for a 600-grooves/mm aluminum-coated grating.[11]

be determined by

$$\rho = \frac{1-\eta}{1+\eta}. \tag{4}$$

We tested seven different reflection gratings with spatial frequencies of 150, 400, 600, 1200, and 5880 grooves/mm in the visible wavelength range. Table 1 lists the measured values of ρ for all seven gratings at three different wavelengths: 543.5, 590, and 632.8 nm.

Figure 2 shows the experimental data points and fitting curve for a 600-grooves/mm aluminum-coated grating[11] at 632.8 nm. The rms error of fitting is ~0.005. The value of ρ is consistent under several measurements, and the standard deviation is ~0.005. Figure 3 shows the real and imaginary parts of ρ as a function of wavelength for the same grating. The results show that the real and imaginary parts of ρ vary significantly over the 25-nm wavelength range. Figure 4 shows the corresponding absolute value and the phase angle of ρ as a function of wavelength for the same grating. The value of $|\rho|$ is nearly constant, whereas the phase angle of ρ shows significant change and reaches almost 90° when λ is slightly >600 nm. This is an interesting result in that at a certain wavelength the zero-order beam reflected from the grating has nearly a quarter-wave differential phase shift. Thus incident linearly polarized light can be reflected circularly polarized under this condition. The results for other gratings show different features for different

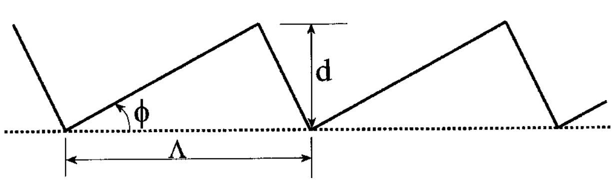


Fig. 5. Assumed profile for the 5880-grooves/mm grating.[12] Λ is the grating period, ϕ is the blaze angle, and $d$ is the groove depth.

**Table 2. Theoretically Calculated ρ for a 5880-grooves/mm Grating[12] at Three Different Wavelengths**

| Groove Depth $d$ (nm) | λ = 543.5 nm | λ = 590 nm | λ = 632.8 nm |
|---|---|---|---|
| 63 | 0.739–$j$0.488 | 0.870–$j$0.428 | 0.912–$j$0.374 |
| 55 | 0.836–$j$0.389 | 0.921–$j$0.332 | 0.946–$j$0.290 |
| Experiment | 0.747–$j$0.318 | 0.932–$j$0.183 | 0.960–$j$0.202 |

grating frequencies and structures over the same wavelength range. The rms error of fitting the $\mathcal{T}_D$ versus θ data (including odd and even harmonics) depends on the intensity stability of the light source and the alignment of the system and varies from 0.015 to 0.025 for the data shown in Fig. 3. The rms fitting error is greater than that obtained with a He–Ne laser source in Fig. 2. The error is caused mainly by the intensity fluctuations of the dye laser output.

## 4. Comparison with Theoretical Calculations for the 5880-grooves/mm Grating

Calculations for the 5880-grooves/mm gold-coated grating[12] were performed by Li using a rigorous grating theory.[6] ρ was calculated at wavelengths of 543.5, 590, and 632.8 nm. The assumed structure of the grating is shown in Fig. 5. The manufacturer specifies a blaze angle ϕ of 24°, and groove depth $d$ of 63 nm. Because the gold-coating thickness is ~1 μm and the grating is nontransmissive at visible wavelengths, it is treated as a pure bulk gold grating regardless of the underlying substrate material. Our grating is a gold-coated replica of a ruled master grating and its groove depth is expected to be ≤63 nm because the manufacturing and coating processes make it difficult to maintain exactly the same groove profile as that of the master. ρ was calculated at two groove depths of 63 and 55 nm for comparison. The complex refractive index of gold was obtained by interpolation using known values at the nearest wavelengths from Refs. 13, 14, and 15, which gives 0.3867–$j$2.5941, 0.2360–$j$3.0740, and 0.1829–$j$3.3885 at wavelengths of 543.5, 590, and 632.8 nm, respectively. The calculated results appear in Table 2. The smaller groove depth gives better agreement between the calculated and measured ρ. The agreement between the calculated and measured values of ρ can be improved by making further minor adjustments of the groove shape, groove depth, and the optical constants of the gold coating.[16] As these preliminary results indicate, combining the NIRSE measurements of the ratio of complex reflection coefficients ρ and rigorous grating theory gives a useful tool for determining at least some of the grating parameters. The NIRSE can be operated over the broader spectrum of a continuum source by replacing detector $D_1$ with an appropriate spectrometer.

## 5. Conclusion

Experimental results of ratios of complex reflection coefficients ρ at normal incidence for different gratings as measured by the NIRSE have been presented. The results of ρ versus wavelength show some interesting features. When used in conjunction with grating theory, the NIRSE provides a useful new tool for the characterization of surface-relief gratings.

We are grateful to Lifeng Li of the Optical Sciences Center, University of Arizona, for performing the calculations reported in Table 2. This research was supported by the National Science Foundation.

## References and Notes

1. R. M. A. Azzam, "PIE: perpendicular-incidence ellipsometry-application to the determination of the optical properties of uniaxial and biaxial absorbing crystals," Opt. Commun. **19,** 122–124 (1976).
2. R. M. A. Azzam, "NIRSE: normal-incidence rotating-sample ellipsometer," Opt. Commun. **20,** 405–408 (1977).
3. P. S. Hauge, "Recent development in instrumentation in ellipsometry," Surf. Sci. **96,** 108–140 (1980).
4. R. Petit, ed., *Electromagnetic Theory of Gratings* (Springer-Verlag, Berlin, 1980), Chaps. 3 and 4.
5. T. K. Gaylord and M. G. Moharam, "Analysis and applications of optical diffraction by gratings," Proc. IEEE **73,** 894–938 (1985).
6. J. Chandezon, M. T. Dupuis, G. Cornet, and D. Maystre, "Multicoated gratings: a differential formalism applicable in the entire optical region," J. Opt. Soc. Am. **72,** 839–846 (1982).
7. L. Li, "Multilayer modal method for diffraction gratings of arbitrary profile, depth, and permittivity," J. Opt. Soc. Am. A **10,** 2581–2591 (1993).
8. Coherent Innova-70 ar-ion laser and CR-599 dye laser system (Coherent Laser Group, Palo Alto, Calif.).
9. R. M. A. Azzam, "Stationary property of normal-incidence reflection from isotropic surfaces," J. Opt. Soc. Am. **72,** 1187–1189 (1982).
10. D. C. Nick and R. M. A. Azzam, "Performance of an automated rotating-detector ellipsometer," Rev. Sci. Instrum. **60,** 3625–3632 (1989).
11. Spectrogon US, Inc., Parsippany, N.J.
12. David Richardson Grating Laboratory (formerly Milton Roy Co.), Rochester, N.Y.
13. L. G. Schulz, "Optical constants of silver, gold, copper, and aluminum. I. The absorption coefficient *k*," J. Opt. Soc. Am. **44,** 357–368 (1954).
14. G. Haas and L. Hardley, "Optical properties of metals," in *American Institute of Physics Handbook,* D. E. Gray, ed. (McGraw-Hill, New York, 1972), 6-118–6-169.
15. M. A. Ordal, L. L. Long, R. J. Bell, S. E. Bell, R. R. Bell, R. W. Alexander, Jr., and C. A. Ward, "Optical properties of the metals Al, Co, Cu, Au, Fe, Pb, Ni, Pd, Pt, Ag, Ti, and W in the infrared and far infrared," Appl. Opt. **22,** 1099–1119 (1983).
16. It is possible to obtain independent information about the surface profile using techniques such as atomic-force microscopy and to measure the optical constants of the deposited gold film on an optical flat during the same coating cycle used to prepare the grating.
17. American Holographic, Inc., Littleton, Mass.